

“ECCO Follow-On: Understanding Sea Level, Ice, and Climate”

Ichiro Fukumori¹, Ian Fenty¹, Gael Forget², Patrick Heimbach³, Chris Hill²,
Dimitris Menemenlis¹, Rui Ponte⁴ & Carl Wunsch²

¹Jet Propulsion Laboratory, Caltech, Pasadena, CA, ²Massachusetts Institute of Technology, Cambridge, MA,
³University of Texas, Austin, TX, ⁴Atmospheric and Environmental Research, Lexington, MA,

Overview

The Consortium for Estimating the Circulation and Climate of the Ocean (ECCO) has provided ongoing global multi-decadal estimates of the physical state of the ocean. Results are characterized by their physical and statistical consistencies, which make them particularly suitable for investigating mechanisms of ocean circulation [see poster by Ponte *et al.*]. An effort is underway to advance the estimate to study Earth's climate with a focus on improving understanding and prediction of global sea level change. The effort is a direct successor to the ongoing ECCO-Production and ECCO-IcES projects and will incorporate capabilities for coupled ocean, ice sheet, and sea ice estimation.

Multi-Decadal Estimates

The latest multi-decadal ECCO solution, referred to as ECCO Version 4 Release 1 (hereafter v4r1) [1], synthesizes nearly all extant data of the global ocean since 1992 (Table 1). By using a grid that is analogous to a cubed-sphere (Fig. 1), the domain includes the Arctic Ocean and is now truly global. The estimate (Fig. 2) is also characterized by its employment of a partial-cell rescaled (z^*) vertical coordinate [2] and a nonlinear free surface boundary condition with real freshwater fluxes [3]. These advancements allow accurate representation of topography as well as undulations in the free surface under ice [4] and achieve complete conservation of fresh water, heat and salt. These characteristics are critical for estimating ocean-ice interaction and for attribution and process studies of climate change. The estimate is further being extended in time and in scope as a revised solution (Release 2; v4r2) by incorporating additional observations (Table 1), improved parameterizations (e.g., sea ice), and expanded controls (e.g., initial u, v, η). Prior error estimates (weights) are also revised with updated estimates and by taking account of the model's inhomogeneous grid and temporal correlation, which otherwise can bias the optimization (Eq. 1).

Eq. 1: ECCO v4 minimizes weighted model (x)-data (y) misfits along with the controls (c) consistent with the model (F).

$$J = \sum_i (y_i - Hx_i)^2 / \sigma_y + \sum_i c_i^2 / \sigma_c + \sum_i \lambda_i (x_{i+1} - F(x_i, c_i))^2$$

Interactions with Ice Sheets and Sea Ice

Ocean interactions with the Greenland and Antarctic ice sheets will be incorporated into the Central Production. These will initially be in parameterized form based on thermodynamic ice shelf cavity and calving front modules that have been developed for Antarctica [5] (Fig. 3) and Greenland [6]. The estimate will subsequently employ a novel multi-level nesting scheme that treats downscaling and upscaling between the coarse global-scale model and a series of fine regional-scale models as a joint estimation problem [see poster by Fenty and Fukumori]. Ocean state estimation with a full dynamic ice sheet model is beyond the immediate scope of this effort, but will be explored pending development by partner efforts [7].

To better estimate fluxes of energy and mass modulated by sea ice, we will also employ a thermodynamic/dynamic sea ice model and its adjoint [8]. The model supports multiple ice rheologies and solver approaches that improve convergence [9] and has been used to study Arctic sea ice sensitivity to atmospheric forcing [10] and in an ocean and ice state estimate of the Arctic region [11] (Fig. 4).

Causal Mechanisms and the Model Adjoint

As a measure of sensitivity, model gradients that adjoints can efficiently evaluate provide a means to identify the ocean's controlling mechanisms and are effective tools for studying the ocean. For instance, to first approximation, any model quantity of interest, J , can be expanded in terms of its controls/forcing (c) using the adjoint gradients ($\partial J / \partial c$) [12] (Fig. 5):

$$J(t) \approx \sum_i \sum_x \sum_{\Delta t} \frac{\partial J}{\partial c_i(x, \Delta t)} \delta c_i(x, t - \Delta t) \quad \text{Equation 2: Adjoints can be used to expand quantities of interest.}$$

The largest term on the right hand side identifies the dominant control that dictates J . The MITgcm employed in ECCO is one of the few ocean general circulation models for which adjoints are routinely derived. The new ECCO Follow-On effort will make the ECCO adjoint available for general application by use of the new open-source Automatic Differentiation (AD) tool, OpenAD [13]. Furthermore, a novel generic formulation will be employed such as to allow adjoint applications without expertise in utilizing AD tools.

Summary

In response to a growing demand on the fidelity and scope of ocean state estimation, the ECCO multi-decadal estimate is being advanced to address a wider range of topics in ocean climate variability and to foster a broader utilization of its estimates and modeling system. Of particular interest is the understanding and prediction of global sea level rise. ECCO's comprehensive synthesis and theoretical rigor provide a unique framework to address this problem. The advancements also aim to improve the usability of ECCO's products as a facility for ocean analysis in support of the broader climate community.

References

1. Forget *et al.*, (2015), *Geosci. Model Dev.*, **8**(5), 3653-3743.
2. Adcroft and Campin (2004), *Ocean Modelling*, **7**(3-4), 269-284.
3. Campin *et al.*, (2004), *Ocean Modelling*, **6**(3-4), 221-244.
4. Campin *et al.*, (2008), *Ocean Modelling*, **24**(1-2), 1-14.
5. Schodlok *et al.*, (2015), *J. Geophys. Res.*, (submitted).
6. Sciascia *et al.*, (2014), *J. Geophys. Res.*, **119**(10), 7078-7098.
7. Larour *et al.*, (2014), *The Cryosphere*, **8**, 2335-2351.
8. Fenty and Heimbach (2013), *J. Phys. Oceanogr.*, **43**(5), 884-904
9. Losch *et al.*, (2014), *J. Comput. Phys.*, **257**(PA), 901-911.
10. Koldunov *et al.*, (2013), *Clim Dynam*, **41**(2), 227-241.
11. Fenty *et al.*, (2015), *Clim. Dyn.*, (submitted).
12. Fukumori *et al.*, (2015), *Prog Oceanogr*, **134**(0), 152-172.
13. Heimbach *et al.*, (2011), *Deep Sea Res. Part II*, **58**(17-18), 1858-1879.

Acknowledgment

This work was carried out at the Jet Propulsion Laboratory, California Institute of Technology, under a contract with the National Aeronautics and Space Administration (NASA).

Variable	Source (Duration) / Reference (Year)
Sea level anomaly	TOPEX/Poseidon, Jason-1 & -2 (1992-2013), Geosat-Follow-On (2001-2005), ERS-1/2 (1992-2001), ENVISAT (2002-2008).
Time-mean SSH	GRACE (2002-2013), altimetry (1992-2013)
Global mean SL & OBP	GRACE (2002-2013), altimetry (1992-2013)
OBP anomaly	GRACE (2002-2013)
Temperature	CTDs (1992-2013), XBTs (1992-2013), Argo floats (1997-2013), TOGA/TAO+PIRATA moorings (1992-2013)
Salinity	CTDs (1992-2013), Argo floats (1997-2013)
SST	AVHRR (1992-2013), TMI (1998-2013), AMSR-E (2002-2013)
SSS	Aquarius (2011-2015)
climatology (T&S)	Gouretski and Koltermann (2004)
Key transports	Florida Strait transport (1992-2013)
Sea ice concentration	SSM/I (1992-2013)

Table 1: Observations employed (v4r2 extensions in red).

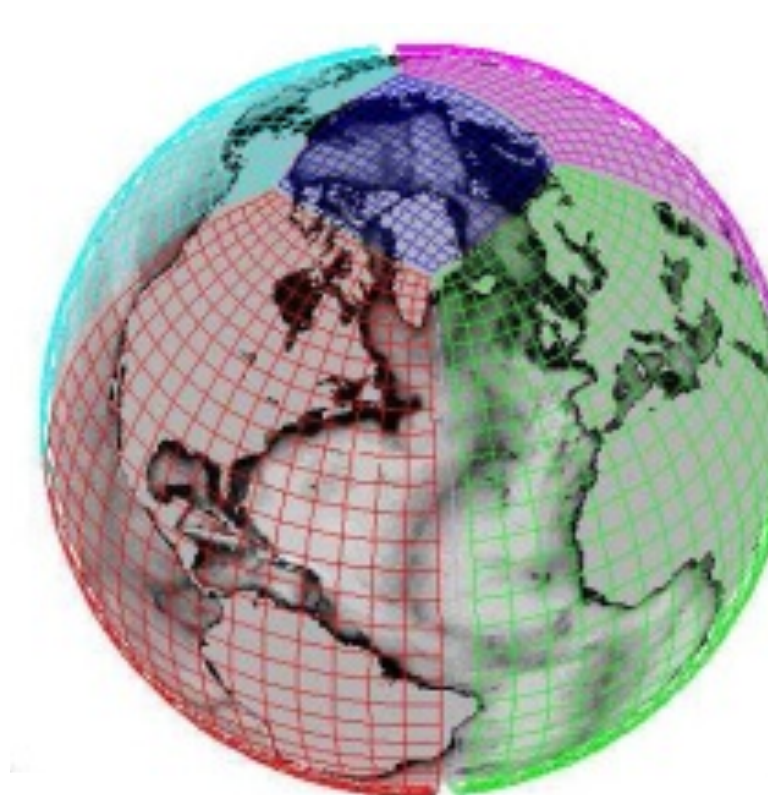


Figure 1: Model grid of v4.

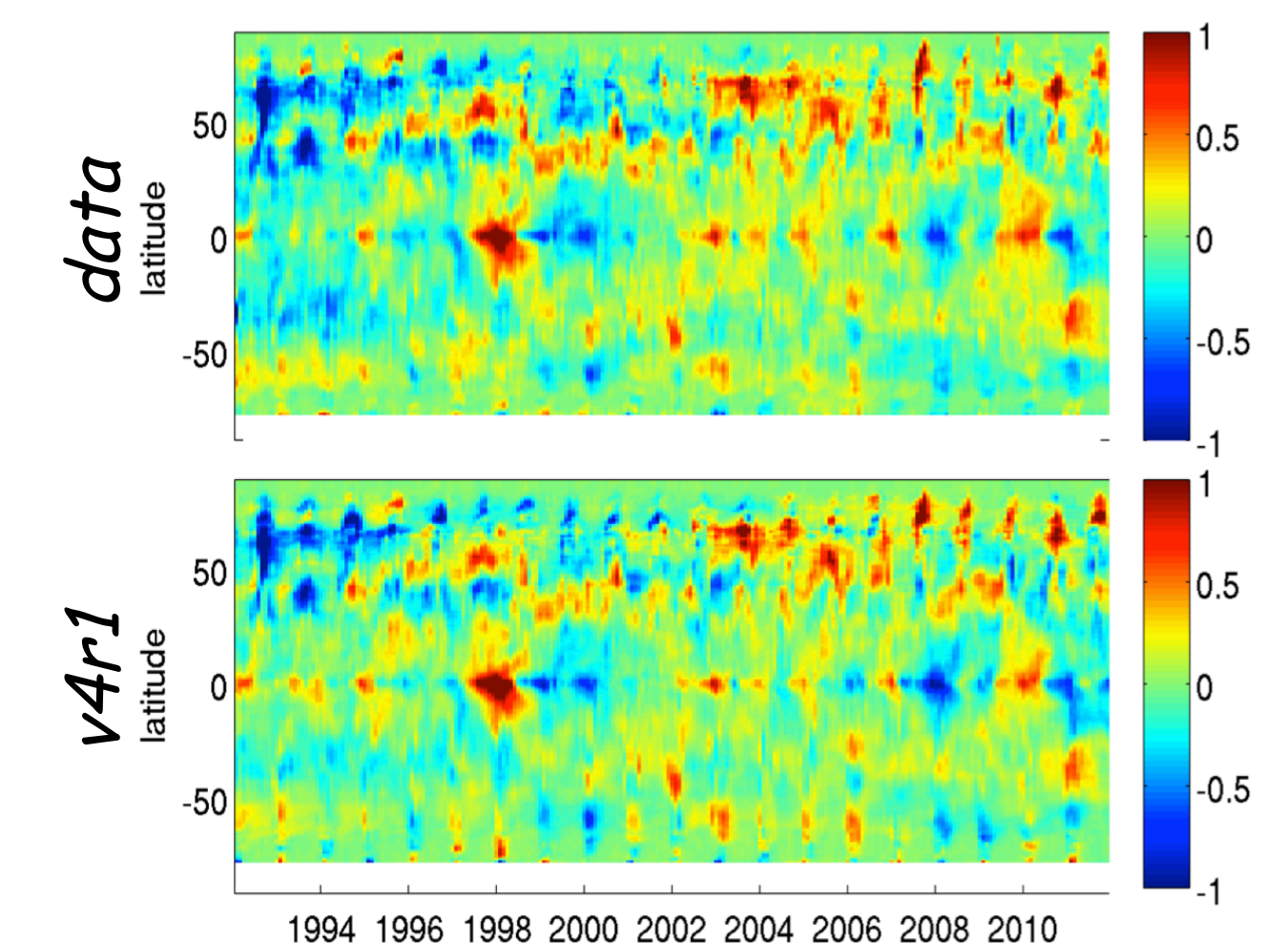


Figure 2: Zonal mean SST anomalies (°C) illustrating skill of v4r1 [1].

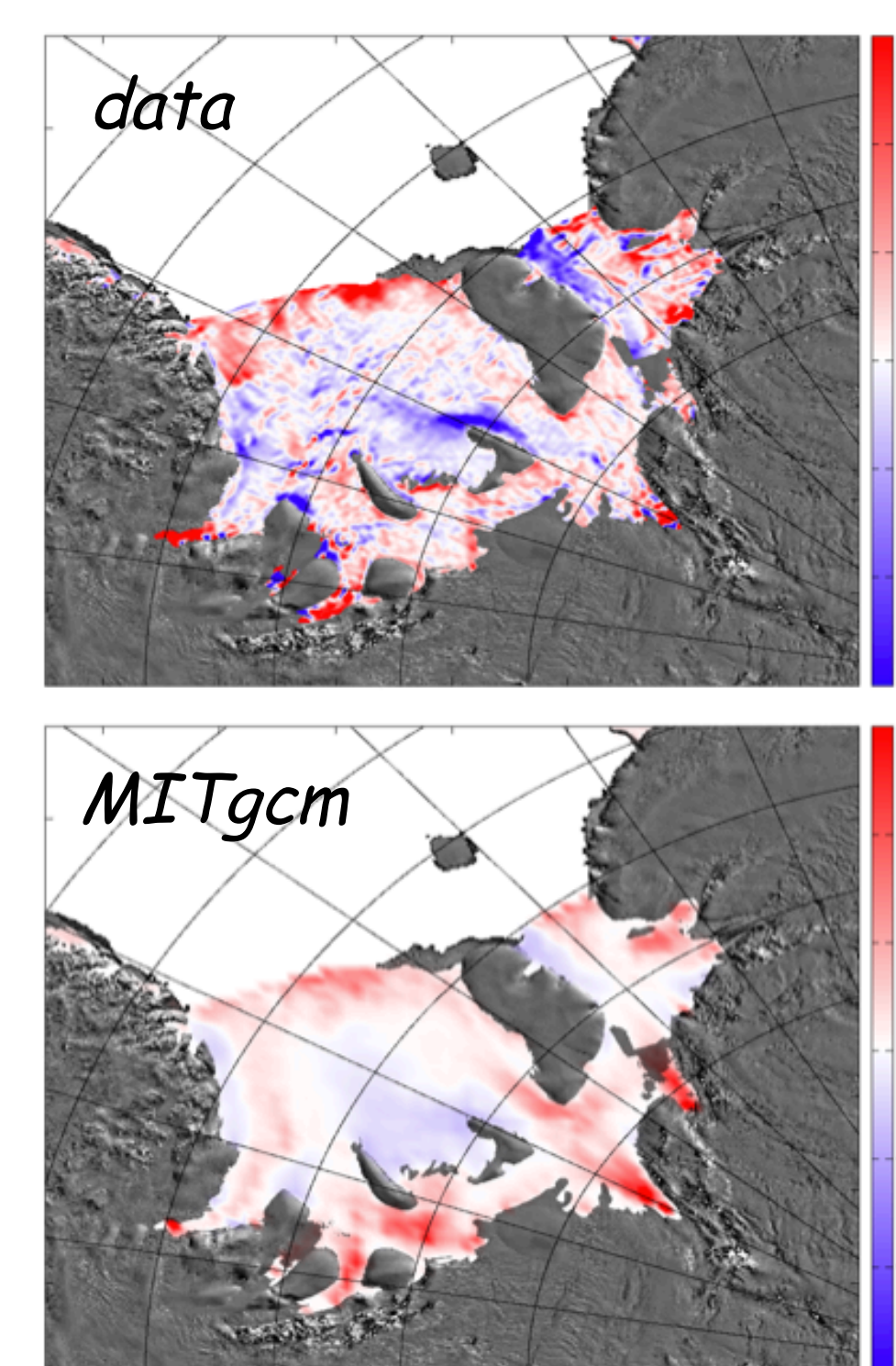


Figure 3: Mean basal melt rate (m/a) for Filchner Ronne Ice Shelf [5].

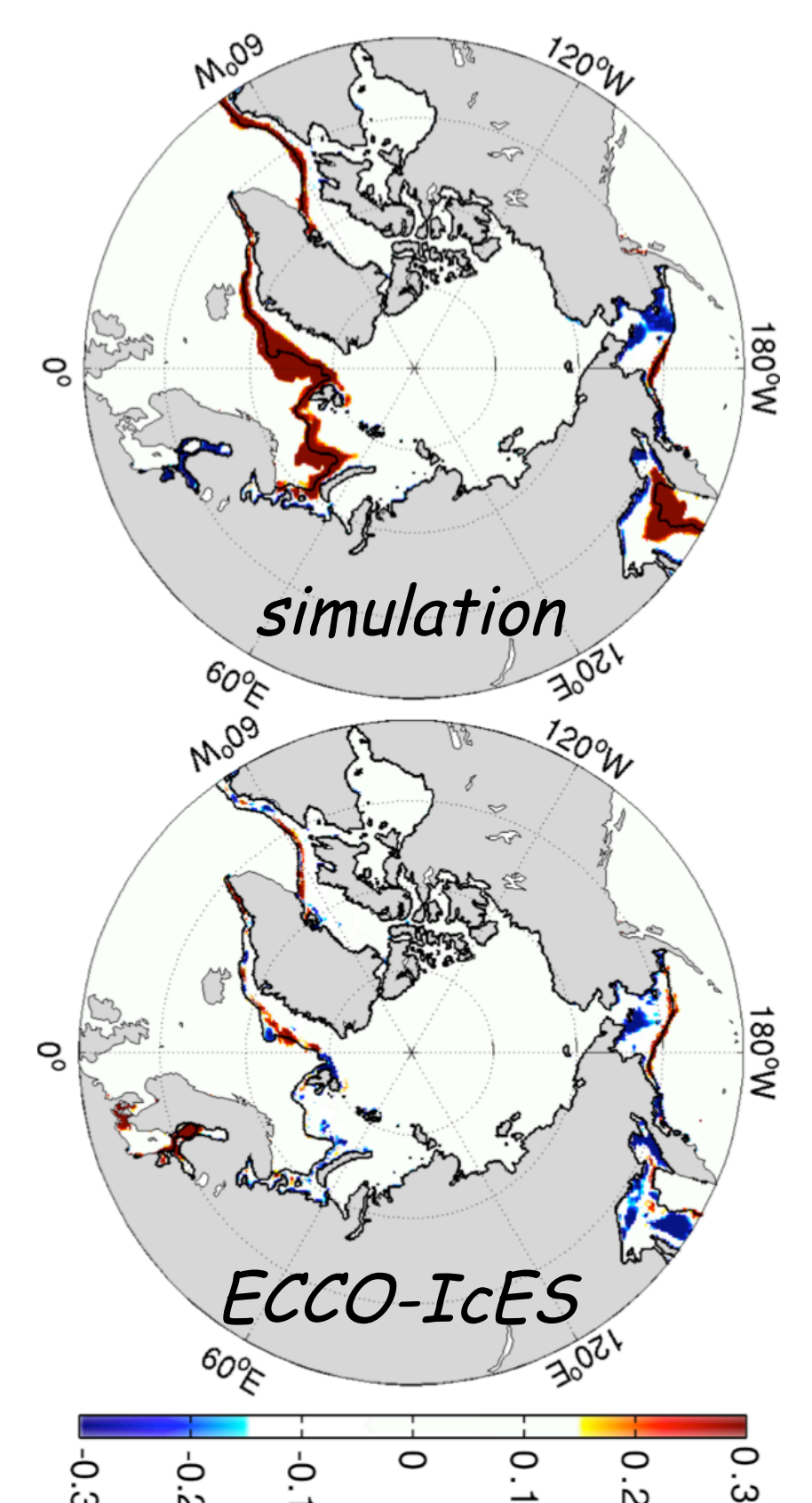


Figure 4: Model-data difference of sea ice concentration (March) [11].

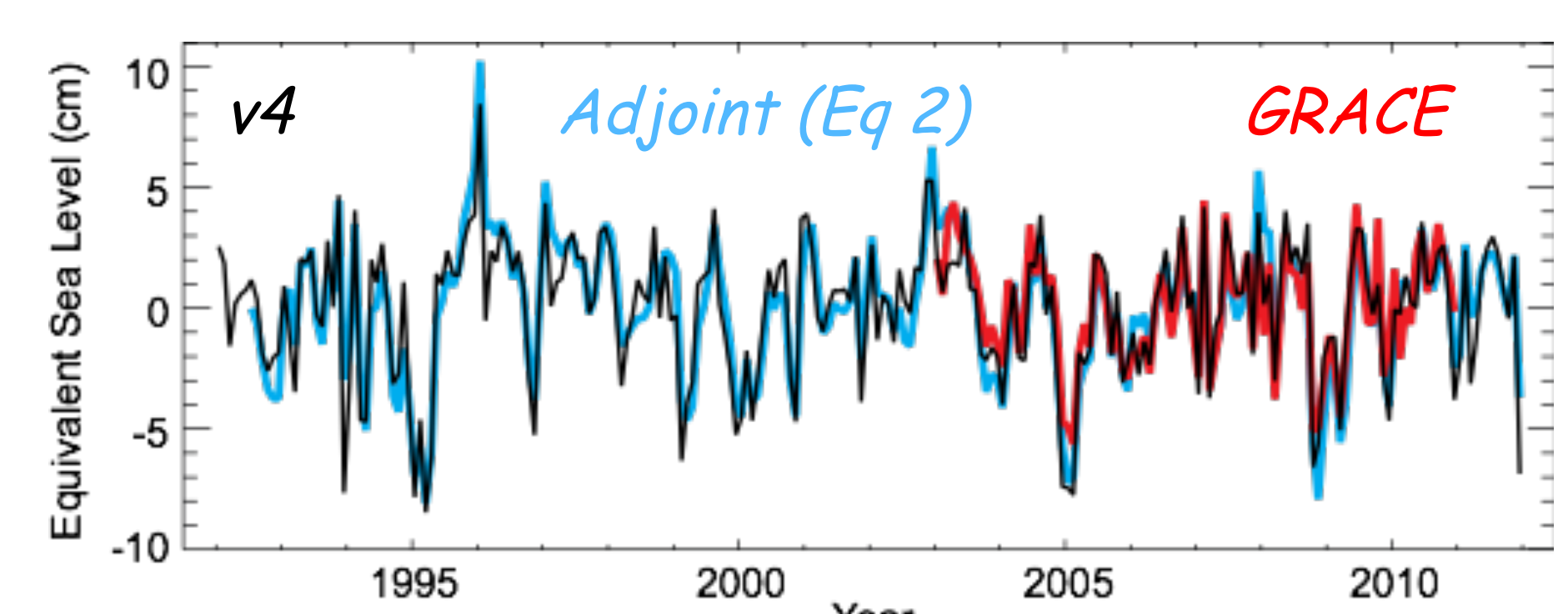


Figure 5: Mean ocean bottom pressure of the Arctic Ocean [12].